Plant Mol Biol (2011) 77:185–201
DOI 10.1007/s11103-011-9802-0

Down-regulation of free riboflavin content induces hydrogen peroxide and a pathogen defense in *Arabidopsis*

Benliang Deng · Sheng Deng · Feng Sun · Shujian Zhang · Hansong Dong

Received: 12 June 2010 / Accepted: 8 June 2011 / Published online: 1 July 2011

Abstract Riboflavin mediates many bioprocesses associated with the generation of hydrogen peroxide (H_2O_2), a cellular signal that regulates defense responses in plants. Although plants can synthesize riboflavin, the levels vary widely in different organs and during different stages of development, indicating that changes in riboflavin levels may have physiological effects. Here, we show that changing riboflavin content affects H_2O_2 accumulation and a pathogen defense in *Arabidopsis thaliana*. Leaf content of free riboflavin was modulated by ectopic expression of the turtle gene encoding riboflavin-binding protein (RfBP). The *RfBP*-expressing *Arabidopsis thaliana* (REAT) plants produced the RfBP protein that possessed riboflavin-binding activity. Compared with the wild-type plant, several tested REAT lines had >70% less flavins of free form. This change accompanied an elevation in the level of H_2O_2 and an enhancement of plant resistance to a bacterial pathogen. All the observed REAT characters were eliminated due to *RfBP* silencing (RfBPi) under REAT background. When an H_2O_2 scavenger was applied, H_2O_2 level declined in all the plants, and REAT no longer exhibited the phenotype of resistance enhancement. However, treatment with an NADPH oxidase inhibitor diminished H_2O_2 content and pathogen defense in wild-type and RfBPi but not in REAT. Our results suggest that the intrinsic down-regulation of free flavins is responsible for NADPH oxidase-independent H_2O_2 accumulation and the pathogen defense.

Keywords *Arabidopsis thaliana* · Hydrogen peroxide · Pathogen defense · Riboflavin (RIB) · Riboflavin-binding protein (RfBP)

Benliang Deng, Sheng Deng, Feng Sun, and Shujian Zhang have contributed equally to this work.

Electronic supplementary material The online version of this article (doi:10.1007/s11103-011-9802-0) contains supplementary material, which is available to authorized users.

B. Deng · S. Deng · F. Sun · S. Zhang · H. Dong (✉)
State Ministry of Education Key Laboratory of Integrated Management of Crop Pests, Nanjing Agricultural University, Nanjing 210095, China
e-mail: hsdong@njau.edu.cn

S. Deng · F. Sun
Institute of Plant Protection, Jiangsu Province Academy of Agricultural Sciences, Nanjing 200014, China

S. Zhang
Plant Pathology Department, University of Florida, Gainesville, FL 32611, USA

Introduction

Flavins have three major forms, riboflavin (RIB), or vitamin B_2; flavin mononucleotide (FMN); and flavin adenine dinucleotide (FAD) (Weimar and Neims 1975; Powers 2003). RIB is the precursor of FMN and FAD, essential cofactors for many metabolic enzymes in multiple cellular processes, such as the citric acid cycle and cellular redox (Jordan et al. 1999). Flavin-mediated redox is critical (Gajewska and Sklodowska 2007) for the generation of reactive oxygen species (ROS) of different types (Torres et al. 2006; Fernandez and Strand 2008), such as superoxide anion ($O_2^{\bullet -}$) (Piacenza et al. 2007; Deng et al. 2010) and the more stable hydrogen peroxide (H_2O_2) (Ashtamker et al. 2007; Torres 2010; Paranagama et al. 2010).

H_2O_2 is a cellular signal that mediates multiple bioprocesses and accumulates frequently in coordination with defense responses in plants (Orrenius et al. 2007; Torres 2010). Recently we summarized previous studies that

suggest either dispensable or indispensable roles of H_2O_2 for defense responses under different conditions (Wang et al. 2009). Defense responses often accompany the accumulation of H_2O_2, but causal relationships between both events vary with circumstances. In plants under infection by pathogens or those treated with elicitors, H_2O_2 is either indispensable (Levine et al. 1994; Trouvelot et al. 2008; Zhang et al. 2009) or dispensable (Sasabe et al. 2000; Binet et al. 2001; Peng et al. 2003, 2004) for defense responses. We have shown that plant resistance to pathogens is induced by the extrinsic application of RIB (Dong and Beer 2000) and H_2O_2 is necessary (Zhang et al. 2009).

It is unclear whether the changes in intrinsic RIB content affect H_2O_2 production and defense responses in plants. Although plants can synthesize RIB, levels vary widely in different organs and during different stages of development (Weimar and Neims 1975; Sierra and Vidal-Valverde 1999), suggesting that changes in RIB levels may have physiological effects (Mori and Sakurai 1996). Foliar application of RIB induces defense responses to pathogens (Dong and Beer 2000; de Souza et al. 2006; Taheri and Höfte 2006; Zhang et al. 2009; Taheri and Tarighi, 2010). In *Arabidopsis thaliana* (*Arabidopsis*), extrinsically applied RIB induces defense responses with the accumulation of H_2O_2 under bacterial pathogen infection (Zhang et al. 2009). However, the extrinsic application of RIB to plants might not duplicate the functions of intrinsically generated RIB. Therefore, we sought to manipulate intrinsic RIB content by engineering plants with an animal gene that encodes the RIB-binding protein (RfBP).

RfBP is a phosphoglycoprotein that was first isolated from the white of chicken egg (Rhodes et al. 1959). So far, the protein has been identified in other oviparous species in addition to chicken (Maehashi et al. 2009), amphibian (Storey et al. 1999), fish (Wang et al. 2003), and mammals (Natraj et al. 1988). In ovipara, the *RfBP* gene is expressed in the liver and the oviduct in an estrogen-dependent manner, and in oocytes subsequent to fecundation (Hamajima and Ono 1995; Zheng et al. 1988; Maehashi et al. 2009). The estrogen-dependent and fecundation-induced expression patterns are also found in other animals (Storey et al. 1999; Natraj et al. 1988; Wang et al. 2003). RfBP is mainly produced in the blood plasma of podocyte and binds to the plasma membrane via a ligand binding domain located in the N-terminal region of RfBP sequence (Monaco 1997; Latha et al. 2008). RfBP also has a C-terminal phosphorylated domain that accommodates the RIB molecule and enables RfBP to bind RIB tightly in a 1:1 molar ratio (Monaco 1997; Kozik 1982; Bartosík et al. 2009). Owing to the structural features, RfBP plays a role in the subcellular translocation of RIB in the animals (Huang and Swaan 2000; Foraker et al. 2003). The animals absorb RIB directly from dietary sources (Gastaldi et al. 1999) or produce RIB through conversions from ingested FMN and FAD (Powers 2003; Said and Mohammed 2006). In both cases, RfBP acts to redistribute RIB between cells and organs (Huang and Swaan 2000; Latha et al. 2008). During embryo development in the animal, RfBP uses a ligand-receptor binding manner (Adiga et al. 1988; Wasylewski 2000; Latha et al. 2008) to mediate RIB translocation to the growing embryo (Kozik 1982). Both RIB deficit and insufficient decomposition of the RIB-RfBP complex are fatal to embryogenesis (Sooryanarayana et al. 1998). These findings suggest that RfBP plays an important role in the animal development.

Soft-shelled turtle (*Trionyx sinensis japonicus*) TsRfBP shows a high identity to the chicken (*Gallus domestiaus*) GdRfBP in amino acid sequence, especially in the ligand-binding domain and the phosphorylated domain (Hamajima and Ono 1995; Sabharanjak and Mayor 2004; Bedhomme et al. 2005; Roje 2007). The ligand-binding domain is implicated in the interaction between RfBP and the plasma membrane receptor (Latha et al. 2008). The domain comprises six tryptophane residues in TsRfBP as in GdRfBP (Hamajima and Ono 1995). This feature suggests that both RfBPs bind to the plasma membrane possibly with an equivalent efficiency. On the other hand, the threonine among amino acid residues in the phosphorylated domain is thought to be important for RfBP to bind RIB (Blankenhorn 1978). GdRfBP and TsRfBP both contain eight phosphorylation clusters that comprise nine serine residues and five glutamic acid residues, but TsRfBP has two additional threonine-phosphorylation sites (Hamajima and Ono 1995). This difference suggests that the affinity to RIB may be greater for TsRfBP than GdRfBP.

Based on this consideration, the *TsRfBP* gene was chosen and used in plant transformation to manipulate the intrinsic content of free RIB and presumably FMN and FAD as well. As RIB has the same characters in structure and biochemistry irrespective of organism source, it is possible that TsRfBP binds RIB and thus alters the content of free RIB, FMN or FAD in *TsRfBP*-expressing transgenic plants. This manipulation may have sequent effects on plant defense responses based on biochemical characters of the ligand-binding domain in RfBP. The domain has a fold that appears to be strongly conditioned by the presence of nine disulfide bridges (Monaco 1997) in GdRfBP and in TsRfBP as well (Hamajima and Ono 1995). The insertion of disulfide bridges into the unfolded form of reduced RfBP is catalyzed by the flavin-dependent quiescin-sulfhydryl oxidase, which reduces molecular oxygen to form H_2O_2 (Rancy and Thorpe 2008). This channel of H_2O_2 generation should add to the enzymatic dismutation of $O_2^{\cdot-}$ generated by NADPH oxidases on the plasma membrane (Ashtamker et al. 2007; Deng et al. 2010; Torres 2010). In *TsRfBP*-expressing transgenic plants, H_2O_2 may be

generated from the two membrane-associated sources to affect defense responses as a result of the modulation for the intrinsic RIB content. In plants, however, the RIB biosynthesis pathway (Bacher et al. 2001; Roje 2007) is required for various physiological processes (Weimar and Neims 1975; Asai et al. 2010). Mutagenicity at the pathway may be lethal to plants or produce mutants with impaired RIB biosynthesis and ambiguous phenotypic modifications (Xiao et al. 2004). In addition, there were two additional considerations for the experimentation. The induction of *TsRfBP* expression in turtle by treatment with an estrogen allows for convenient gene cloning (Hamajima and Ono 1995). The absence of RfBP homologs in the plant kingdom, including the completely sequenced *Arabidopsis* genome (Lorenz et al. 2003), clears the atmosphere in regard to gene silencing and undesired effects under the condition of ectopic *TsRfBP* expression in transgenic plants. Therefore, we adopted transgenic and gene-silencing methods, respectively, to manipulate ectopic expression and silencing of the *TsRfBP* gene in *Arabidopsis*. We investigated subsequent effects of both engineering approaches on the intrinsic levels of flavins and H_2O_2 in correlation with plant resistance to *P. syringae* pv. *tomato*.

Materials and methods

Plants and bacteria

Wild-type (WT) and transgenic plants of *Arabidopsis* ecotype Col-0 were grown in an environment-controlled chamber (Dong et al. 2005). Plants used in transformation were grown in long day (16-h light/8-h dark) till flowering. In other experiments, plants were grown in short day (12-h light/12-h dark) for 35 d before use. Bacteria *Escherichia coli* and *Agrobacterium tumefaciens* were used in the production of TsRfBP and plant transformation, respectively. The bacterial pathogen used in the test of the plant defense response was *P. syringae* pv. *tomato* strain DC3000 (hereafter referred to as DC3000). Bacteria were maintained and multiplied as described (Dong et al. 1999; Peng et al. 2004).

Vectors

The pET30a(+) vector (Novagen) was used for gene cloning and prokaryotic expression. The vector contains two copies of six tandem histidines (His-tag) and the left one was removed before use in this study (Chen et al. 2008). The binary pBI121 vector (Clontech) containing the cauliflower mosaic virus 35S promoter (35S) was used in plant transformation. The pBSSK-in vector (Stratagene) was used to construct the hairpin-based *TsRfBP*-silencing unit. This vector contains a 200-bp intron, a hygromycin-resistance gene (*HYG*), and a β-glucuronidase reporter gene (*uidA*).

Preparation and purification of the TsRfBP-His fusion protein

Total RNA was isolated from livers of *T. sinensis japonicus* mature females, which had been injected with an aqueous solution of 10 μg/ml estrone and incubated under room temperature for 24 h (Hamajima and Ono 1995). RNA sample was subjected to reverse transcriptase-polymerase chain reaction (RT–PCR) using specific primers (Table 1) to yield 729-bp full length *TsRfBP* cDNA. Sequence-confirmed *TsRfBP* was cloned into pET30a(+), creating pET30a(+)::*TsRfBP-his*, followed by transformation of *Escherichia coli* BL21 (DE3). Transformed BL21 cells were cultured to produce the TsRfBP-His fusion protein. BL21 cells transformed with pET30a(+)::*his* were incubated to produce control protein preparation PET. Protein preparations were purified by nickel chromatography (Chen et al. 2008) using the HisTrap HP Kit including the HiTrap nickel column (Amersham). The column was saturated with 10 ml imidazole-binding buffer (10 mM, pH 7.4), and proteins were loaded and eluted with 10 mM phosphate buffer containing various concentrations of imidazole. Proteins were resolved by tricine-sodium dodecyl sulphate–polyacrylamide gel electrophoresis (T-SDS-PAGE).

Antibody preparation and immunologic assays

Polyclonal TsRfBP antibody was produced by immunizing New Zealand white rabbit (*Oryctolagus cuniculus*) with the TsRfBP protein made from the prokaryotic expression system and purified by nickel chromatography. TsRfBP of 1 mg/ml was emulsified thoroughly in equal volume of Freund's complete adjuvant and Freund's incomplete adjuvant (Sigma), respectively. Rabbit was immunized by nape hypodermic with Freund's complete adjuvant/NtTRXh3 emulsion, followed by consolidated immunization conducted 2 weeks later and using Freund's complete adjuvant/NtTRXh3 emulsion. The consolidated immunization was done every 2 weeks and for 2–3 times depending on the antiserum titer determined by ELISA. The GdRfBP protein was from a commercial source (Sigma) and the polyclonal GdRfBP antibody was produced similarly as for polyclonal TsRfBP antibody. Cross reactions were also determined by the double immunediffusion and ELISA. ELISA was done using goat anti-rabbit IgG-HRP and companion reagents according to instructions from the vender (Beyotime Inst. Biotech., Haimen, China).

Table 1 Information on genes tested in this study

Gene	GenBank accession no.	Primers	Product size (bp)	Tests
TsRfBP	TYXRBPSP	5′-CGGGATCCATGTTCAAGTCTGTTGCAGTC-3′	729	cDNA cloning, RT–PCR
		5′-TCCCCCGGGTCACAGAATTTCAAACACCT-3′		
		5′-GGCTGACAGATTGGGAATGGGATG-3′	201	Real-time RT–PCR
		5′-TTTCGGAAGTTAAGTACCTGATGG-3′		
		5′-ATGTTCAAGTCTGTTGCAGTCC-3′	460	Silencing construction
		5′-CGTTCTTACAGTGGTTCTCTCC-3′		
HYG	FJ949107	5′-TCCATACAAGCCAACCAC-3′	469	RT–PCR
		5′-TGACCTATTGCATCTCCC-3′		
uidA	AT5G61250	5′-GTCCTGTAGAAACCCCAACCCGTG-3′	588	RT–PCR
		5′-GGTTACAGTCTTGCGCGACATGC-3′		
NTP II	AAL92039.1	5′-ATGATTGAACAAGATGGATTGCACG-3′	790	PCR
		5′-AGAACTCGTCAAGAAGGCGATAGAA-3′		
EF1α	AT1G07930	5′-AGACCACCAAGTACTACTGCAC-3′	469	RT–PCR
		5′-CCACCAATCTTGTACACATCC-3′		
		5′-GCTGATTGTGCTGTCCT-3′	259	Real-time RT–PCR
		5′-CAGAGATGGGCACAAAT-3′		
ACTIN2	NM_112764	5′-CCCCTGAGGAGCACCCAGTTCTA-3′	219	Real-time RT–PCR
		5′-CATACCCCTCGTAGATTGGCACAG-3′		

Fluorescence quenching assay

RIB-binding activity of TsRfBP was determined by the RIB fluorescence quenching assay (Guevara and Zak 1993). The TsRfBP-His fusion protein produced by prokaryotic expression or isolated from REAT was tested using PET and control proteins from WT or TsRfBP-silencing (RfBPi) plants. An aqueous solution containing the mixture of 0.01 μg/ml RIB and a protein preparation of 0.01 μg/ml was incubated under room temperature for 15 min. RIB fluorescence was observed by a microscope under ultraviolet light and quantified with the Hitachi 930 spectrofluorometer.

Generation and characterization of transgenic plants

Full length *TsRfBP* cDNA was obtained from RT–PCR using turtle liver RNA and specific primers (Table 1). The gene was cloned into pET30a(+), creating pET30a(+):: *TsRfBP-his*. The *his* or *TsRfBP-his* fragment was excised from pET30a(+) and inserted into pBI121. For use to construct gene silencing unit, a 460-bp fragment of *TsRfBP* (R_{460}) was obtained by PCR with REAT genomic DNA and *TsRfBP*-specific primers. R_{460} sense and antisense strands were cloned into pBSSK-in by ligation with the intron. The fusion was confirmed by sequencing (Chen et al. 2008). Recombinant pBI121 and pBSSK-in vectors were transferred into *A. tumefaciens* strain EHA105, followed by transformation of Col-0 and a REAT line. Transgenic plants were screened and T3 homozygous progenies were used in this study.

The genomic integration of *TsRfBP* was determined by PCR using the *elongation factor 1 alpha* (*EF1α*) gene as a reference and Southern blot hybridization (Peng et al. 2004). For Southern blots, genomic DNA was digested with *Eco*R I and *Xba* I, and transferred to a nylon membrane, followed by hybridization to a digoxigenin-labeled *TsRfBP* probe prepared using the DIG Nucleic Acid Detection Kit (Roche). The *TsRfBP* silencing effect was tested by RT–PCR analyses of *HYG*, *uidA*, *NTP II*, and *TsRfBP*. Northern blot analysis was done as described (Peng et al. 2004). Proteins used in Western blot analysis were isolated from leaves (Liu et al. 2006) and were purified, quantified, and resolved in gel (Chen et al. 2008). Blots were incubated with the His antibody and horseradish peroxidase-conjugated secondary antibody from the Beyo-ECL Plus Kit (Beyotime Inst. Biotech.), and with the TsRfBP antiserum from immunized rabbits and biotin-labeled secondary antibody (PerkinElmer).

Immunolocalization assay

The subcellular localization of TsRfBP in plants was determined by the immune colloidal gold probing assay and the immune gold-silver double probing assay. For use in both assays, 10-nm colloidal gold particles were tagged to the TsRfBP antiserum by using a previously described protocol (Frens 1973). Plant leaf sections were prepared and treated

according to a protocol established previously by Hodges et al. (1984) and used recently in our studies (Sun et al. 2010; Wu et al. 2010). Plant leaf sections of 1 mm^2 were embedded with the Lowicryl K4 M resin (Cosmo) and polymerized by ultraviolet radiation. Ultrathin sections prepared from the polymerized samples were collected on inert nickel grids in distilled water and then floated on the blocking solution (1% bovine serum albumin; 0.02% polyethylene glycol 20,000; 100 mM NaCl; and 1% NaN_3 in 50 mM phosphate buffer, pH7.0). Blocking reaction was accomplished by incubation under 28°C for 30 min. Blocked samples while carried by inert nickel grids were probed by immersing the grids in a solution of colloidal gold already tagged to the TsRfBP antiserum. Resulting immunogold-probed samples were observed directly or subjected to treatments required for the immune gold-silver probing assay (Holgate et al. 1983). The immunogold-probed samples carried by inert nickel grids were floated on a 0.05 M Tris–HCl buffer solution (pH8.2), washed with highly pure water, and then equilibrated with a 0.05 M citric acid buffer solution (pH3.8). Equilibrated samples were incubated with a silver staining solution under 37°C for 25 min for silver reduction by the gold particles in the samples. The silver staining solution was prepared immediately before use, first by combining aqueous solutions of hydroquinone (1%, v/v) and gum acacia (50%, w/v), and then by combining this mixture with an aqueous solution of silver acetate (0.22%, w/v). These solutions were all prepared with highly pure ion-free water in ion-free glass bottles. The silver acetate solution stock and the silver staining solution were maintained under a light-free condition. The TsRfBP antiserum was used at a 1:20 titer in combination with a 10-nM gold colloid for the immune colloidal gold probing assay and a 1:50 titer in combination with a 5-nM gold colloid for the immune gold-silver probing assay. Samples in both assays were observed by transmission electron microscopy (H-7650; Hitachi, Tokyo).

Reverse transcriptase-polymerase chain reaction (RT–PCR) and real-time RT–PCR

Total RNA was isolated from plant leaves using the Tri Reagent Kit (Sigma). First-strand cDNA was synthesized from 2 μg RNA using the superscript II RNAse H^- Reverse Transcriptase (Invitrogen) and specific primers (Table 1). The *EF1α* gene that has steady expression under most of circumstances (Peng et al. 2003; Liu et al. 2010) was used as a reference. Reaction treatments, RT–PCR protocols, product cloning and sequencing verification were as described (Peng et al. 2003; Dong et al. 2005). RT–PCR products were resolved by agarose gel electrophoresis and visualized by staining with ethidium bromide. An established quantitative method (Livak and Schmittgen 2001) was adopted in real-time RT–PCR using *EF1α*, and *ACTIN2* also, as reference genes since *ACTIN2* is similar to *EF1α* in the steady expression manner (Wu et al. 2010). *TsRfBP* was amplified 26 cycles at a range of template concentration increases by 0.5 ng and from 0 to 3.0 ng in 25 μl reaction solutions to select desired doses. The 25 μl reaction mixture was made of 1 μl tenth-diluted first-strand cDNA, 2.5 μM primer and 1 × SYBR Premix Ex Taq (TaKaRa Biotech. Co., Ltd, Dalian, China). All reactions were performed in triplicates with the null-template control in which *TsRfBP* cDNA was absent. The gene transcript was quantified in relative to those of *EF1α* and *ACTIN2*, respectively. Abundance of the *TsRfBP* transcript from transgenic plants was determined versus the abundance reading from the null-template control.

Flavin measurement

Plant RIB, FMN, and FAD were extracted using extraction Buffer A and Buffer B (Vorwieger et al. 2007). Buffer A was made as an aqueous pH9.6 solution that comprised 5 mM $NaH_2PO_4 2H_2O$, 5 mM $Na_2HPO_4 12H_2O$, 0.2 M NaCl, 0.5 M phenylmethylsulfonyl fluoride, and 1 M ethylene dianetetra-acetic acid. Buffer B was an aqueous pH6.1 solution containing 10% v/v trichloroacetic acid and 0.1 M ammonium acetate solution. Leaf samples were ground on ice with Buffer A and the homogenate was centrifuged at 4°C, 12,000×*g* for 10 min. The supernatant was used to isolate total and free forms of the three flavins. Total flavins were isolated as described (Vorwieger et al. 2007). To isolate free flavins, 500 μl of supernatant was loaded into a Microcon YM-3 (3 kD NMWL) ultrafiltration spin column (Millipore), which was centrifuged at 4°C, 14,000×*g* for 15 min. The flow-through (200 μl) was mixed with Buffer B (1 ml) and centrifuged at 4°C, 12,000×*g* for 10 min. The supernatant contained free flavins. Total or free flavins were filtered through 0.22-μm blend cellulose ester filters (Millipore) and analyzed by high performance liquid chromatography. Concentrations of RIB, FMN and FAD were determined as described (Dawson et al. 1988).

Plant inoculation and pharmacological treatment

Arabidopsis was inoculated by infiltrating 25-μl DC3000 suspension (5 × 10^6 colony formation units per ml) into leaf intercellular spaces at two sites on the 2nd and 3rd expanded leaves using needle-free syringes or spraying plant tops using pressure atomizers. Three and 5 days later, bacterial population in leaf tissues was determined and infection severities were investigated, respectively, using previously described methods (Dong et al. 1999). Catalase, diphenyleneiodonium (DPI), and RIB (Sigma–Aldrich) used in the pharmacological study were prepared as aqueous solutions

(0.5 μU/ml, 5 and 40 μM). They were applied directly or in combination with 100 μM 2, 7-dichlorofluorescein diacetate (DCFH-DA; Amresco), a red dye that emits green fluorescence when oxidized by H_2O_2 and other types of ROS (Allan and Fluhr 1997), by infiltrating leaf intercellular spaces.

ROS detection

The ROS accumulation in plant leaves was visualized by DCFH-DA fluoluminescence assays described in our recent studies (Wang et al. 2009). The content of H_2O_2 in plants was determined by quantifying the plant H_2O_2 extract with a spectrophotometer (Jiang and Zhang 2001). H_2O_2 was extracted from plant leaves (Chen et al. 1993) and quantified by monitoring A_{415} of the titanium-peroxide complex formed with the H_2O_2 extract (Zhang et al. 2009). The content of H_2O_2 in plant leaves was determined according to the A_{415} curve of the titanium-peroxide complex formed with a range of standard H_2O_2 from a commercial source. Subcellular localization of H_2O_2 was detected by fluorescent H_2O_2 probes Amplex Red (AR) and Amplex Ultra Red (AUR) (Invitrogen) as previously described (Ashtamker et al. 2007; Šnyrychová et al. 2009). Both probes were used because previous observations showed that AR and AUR were oxidized in reaction with H_2O_2 to emit strong crimson fluorescence (Ashtamker et al. 2007; Rhee et al. 2010). The excised top second leaves were immediately immersed in the pH7.4 phosphate buffer solution containing 10 μM AR or AUR, and were incubated with the solution in dark for 3 h under a low pressure provided by a vacuum pump and a bell jar. Probed samples were observed under the ZEISS LSM700 laser scanning confocal microscope. The fluorescence emission of oxidized AR and AUR was observed between 585 and 610 nm using 543-nm argon (HeNe) laser excitation.

Data treatment

All experiments were done at least three times with similar results unless specified elsewhere. Quantitative data were applied to Student's *t*-test to evaluate differences caused by the ectopic *TsRfBP* expression compared with the parent (WT) background or caused by a treatment compared with control. Data were also analyzed by *ANOVA* test for comparisons of the plant genotypes (WT, transgenic lines or gene silencing lines) or treatments.

Results

The activity of TsRfBP to bind RIB

The *TsRfBP-his* fusion gene was expressed with a prokaryotic system, producing the TsRfBP-His fusion protein. This protein was compared with commercially obtained GdRfBP in T-SDS-PAGE, which revealed the molecular mass as predicted for TsRfBP-His and GdRfBP being ~35 and ~27 kD, respectively (Fig. 1a). To determine the immunological relationship between both proteins, they were tested in reactions with the TsRfBP antibody and the GdRfBP antibody, respectively. Cross reactions were found in double immunediffusion (Fig. 1b) and ELISA (Fig. 1c) assays. However, the titer determined by ELISA was much higher in reactions of both RfBPs with their own antibodies than cross reactions (Fig. 1c). In a fluorescent quenching assay, the TsRfBP-His fusion protein displayed the RIB-binding activity (Fig. 1d, e; Fig. S1). The activity was detected from the recombinant bacterial cells that contained the protein (Fig. 1d) and the protein preparations from the prokaryotic expression system (Fig. 1e), either unpurified (Fig. 1e) or purified by nickel chromatography (Fig. 1e). These results provided a basis for *TsRfBP* to function once introduced into plants.

Ectopic expression and silencing of the *TsRfBP* gene in *Arabidopsis*

We first generated *TsRfBP*-expressing *Arabidopsis thaliana* (REAT) plants by transformation with the recombinant vector pBI121::*TsRfBP*::*his*. Four REAT lines were selected arbitrarily and characterized in comparison with the transgenic control plant created by transformation of WT *Arabidopsis* with pBI121::*his*. In REAT lines, the *TsRfBP* gene was integrated into the genomes (Fig. 2a), existed as 1–2 copies (Fig. 2b), and was highly expressed (Fig. 2c). The line REAT11 had a single copy (Fig. 2b) and robust expression of *TsRfBP* (Fig. 2d) consistently with abundant TsRfBP protein (Fig. 2e). A greater amount of TsRfBP was detected from REAT11 than from the other three REAT lines (Fig. 2f). In these observations, the transgenic control plant was consistent with the absence of *TsRfBP* gene (Fig. 2a, b), its transcript (Fig. 2c, d), and the TsRfBP protein (Fig. 2e, f), suggesting that the vector itself was not likely to impact the plant characters evaluated in this study. This notion was confirmed in subsequent investigations (Fig. S2a–d). Therefore, the transgenic control plant was no longer shown but WT was used instead in data presentations hereafter.

We next generated *TsRfBP*-silencing (RfBPi) plants by applying a hairpine-based silencing protocol to REAT11 (Fig. 3a). Four RfBPi lines were investigated to evaluate *TsRfBP* silencing effect in comparison with pertinent control genes, *NPT II* and *uidA* from the vector. In contrast to evident expression of *TsRfBP* in REAT11 and evident expression of *NPT II* and *uidA* in both REAT and RfBPi plants, *TsRfBP* transcript in RfBPi plants was not

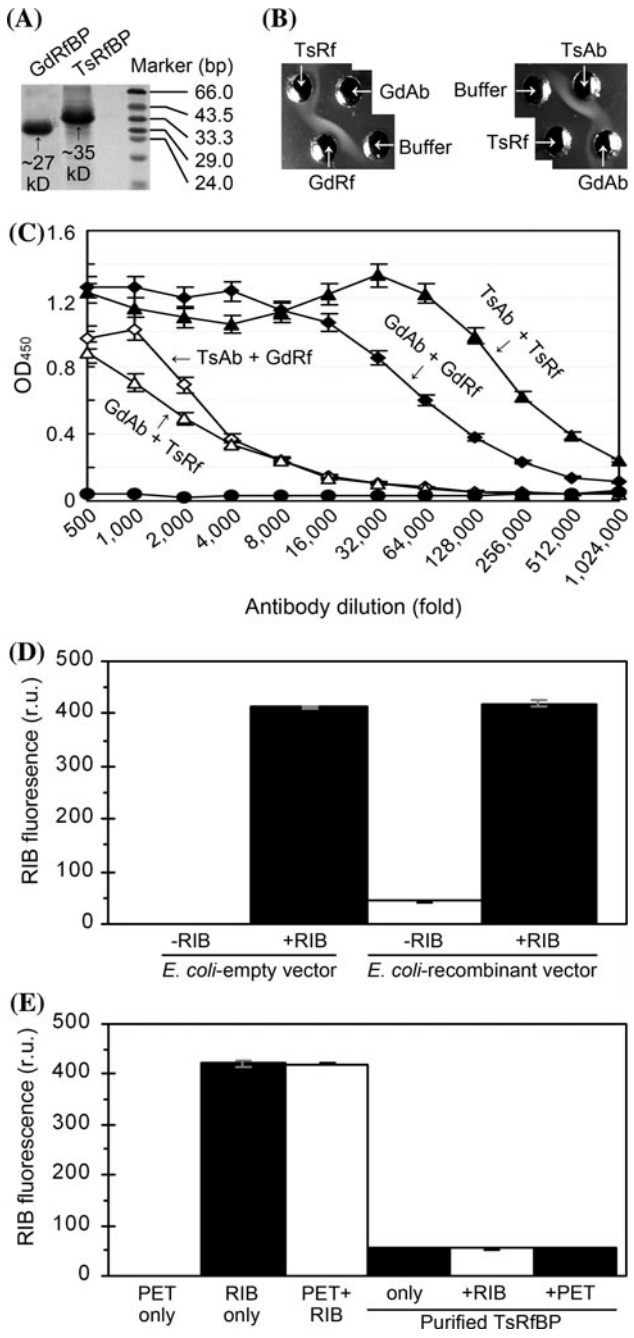

◄ **Fig. 1** Analyses of the turtle (*Trionyx sinensis japonicus*) riboflavin (RIB)-binding protein (TsRfBP) in comparison with the chicken (*Gallus domestiaus*) GdRfBP. **a** The TsRfBP-His fusion protein (TsRfBP) made by prokaryotic expression and purified by nickel chromatography was compared with commercially obtained GdRfBP in tricine-sodium dodecyl sulphate–polyacrylamide gel electrophoresis (T-SDS-PAGE). Marker was used as a reference for the molecular mass, which was predicted as ~35 and ~27 kD for TsRfBP and GdRfBP, respectively. **b** and **c** The double immunediffusion assay (**b**) and ELISA (**c**) were done to determine immunological cross reactions between the RfBPs and their antibodies. TsRfBP-His (TsRf) and GdRfBP (GdRf) were tested in combination with the TsRfBP antibody (TsAb) made by immunizing rabbit and commercially obtained GdRfBP antibody (GdAb), respectively. Phosphate buffer was used as a control in (**b**). In (**c**), titers were evaluated via determining OD450 with a spectrophotometer and presented as means ± standard deviations of results from three experimental repeats. **d** and **e** The RIB fluorescence reading was given as relative unit (r.u.) in contrast to the null reading arbitrarily defined for controls labeled on left of bottom captions. Histograms represent means ± standard (SD) bars of results from three experimental repetitions. Colored images of RIB fluorescence were provided in Fig. S1. **d** RIB fluorescence quenching assays were done using *E. coli* cells transformed with the empty vector and the recombinant vector containing a *TsRfBP* gene insert. **e** RIB fluorescence quenching assays were done using the control protein preparation (PET) produced by *E. coli* cells transformed with the empty vector and TsRfBP-His preparations produced by *E. coli* cells transformed with the recombinant vector

detectable by RT–PCR (Fig. 3b) and was detected at low level by real-time RT–PCR (Fig. 3c). The silencing effect was prominent in the line RfBPi11-1 (hereafter referred to as RfBPi11), which had 92% less *TsRfBP* transcript than REAT11 (Fig. 3c). Abundant amount of the TsRfBP protein was detected in REAT11 but the protein was little in RfBPi11 (Fig. 3d). In addition, TsRfBP remained stable at least for two weeks in the plant protein preparation maintained at 4°C (Fig. S3).

Free flavins are down-regulated due to the ectopic *TsRfBP* expression

As shown in Fig. 4a, total amount of a flavin and the amount of free form of the flavin were determined, and the difference indicated the amount of bound form of the flavin. In REAT11, RIB had a greater amount of bound form but a smaller amount of free form, whereas, both free and bound forms of FMN and FAD were decreased. Free RIB, FMN, and FAD in REAT11 declined to 29, 27, and 23% of WT levels (Student *t*-test, $P < 0.01$). The other three REAT lines were similar to REAT11 in changes of the flavin content. As shown in Fig. 4b, levels of free flavins were much lower in REAT variants than in WT (Student *t*-test, $P < 0.01$), suggesting that down-regulation of free flavin content was a consistent character acquired due to the ectopic expression of *TsRfBP*. This result was confirmed by the *TsRfBP* silencing effect, which restored REAT11 to WT in the character of flavin content. Due to *TsRfBP* silencing, levels of free flavins in RfBPi11 were retrieved to ~90% of those in WT but remained greater than in REAT11 (Fig. 4a). The other three RfBPi lines also had evident restoration of free flavin content to the level of WT (Fig. 4b). In addition, free RIB content declined with plant growth but was still higher in REAT11 than in WT throughout the early, middle, and late growth stages (Fig. S2a). These observations identified REAT11 and RfBPi11 as representative in down-regulated and restored

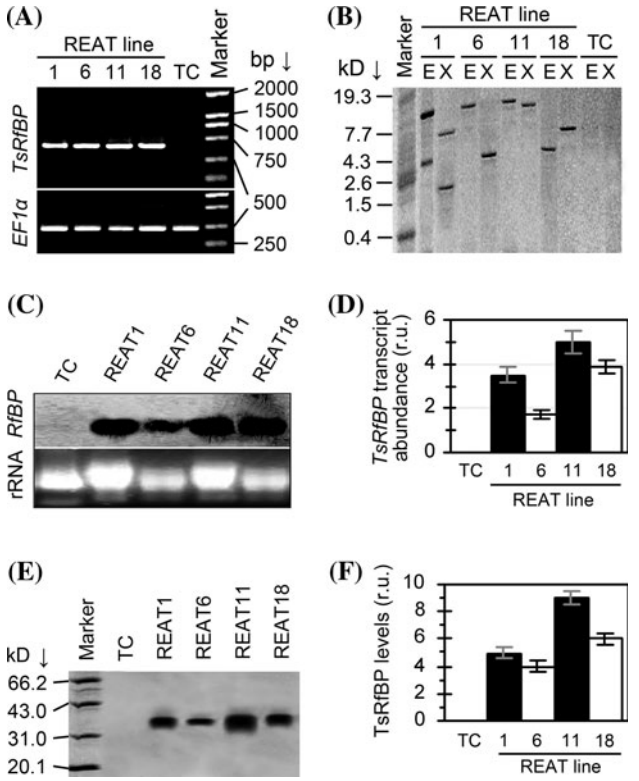

Fig. 2 Characterization of *TsRfBP-his*-expressing *Arabidopsis thaliana* (REAT) generated under the wild-type (WT) background. Coded REAT lines were generated by transformation with the recombinant vector that contained a *TsRfBP::his* insert. For the molecular characterization shown in this figure, the REAT lines were compared with the transgenic control plant (TC) generated by transformation with the vector containing only *his*. **a** PCR analysis of *TsRfBP* using the *EF1α* gene as a reference. **b** Southern blot analyses using specific *TsRfBP* cDNA probe to hybridize with plant genomic DNA that had been digested with restriction enzymes *EcoR* I (E) and *Xba I*(X), respectively. **c** Northern blot analysis using plant RNA and *TsRfBP* cDNA probe. rRNA in gel was visualized by staining with ethidium bromide. **d** Real-time RT–PCR analysis of the *TsRfBP* transcript from the indicated plants. Abundance of the transcript was scored as relative unit (r.u.) in comparison with the abundance reading from the null-template control. Data represent means ± SDs ($n = 3$ repeats; 30 plants/repeat). **e** Western blot hybridized with the TsRfBP antibody and detected with the biotin-labeled secondary antibody. Proteins loaded in gel were isolated from the same amounts of leaf samples for the different plants. **f** Quantification of TsRfBP from plants. Densities of protein bands in gel from (**e**) were quantified with a gel documentation system. The protein level was defined as zero for TC and scored as relative unit (r.u.) for the other plants. Data represent means ± SDs ($n = 3$ repeats; 30 plants/repeat)

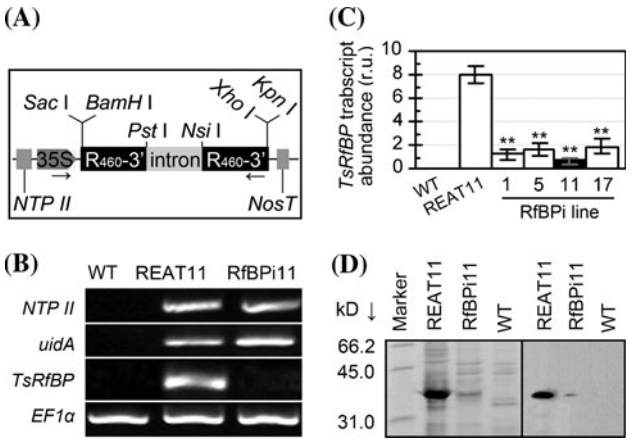

Fig. 3 Characterization of *TsRfBP*-silencing (RfBPi) plants created under the REAT11 background. **a** A part of *TsRfBP*-silencing unit. R_{460} refers to a 460-bp fragment of *TsRfBP*. The *HYG* and *uidA* genes were not silencing and were used as controls to test *TsRfBP*-silencing effect in (**b**). The *uidA* gene is located at the right terminus and is not shown. **b** Evaluation of *TsRfBP*-silencing effect by RT–PCR analyses of *HYG* and *uidA* using plant RNA and specific primers and using *EF1α* as a standard. **c** Real-time RT–PCR analysis using *TsRfBP*-specific primers and template of cDNA synthesized from plant RNA. Products were quantified relative to the null-template control. Data represent means ± SDs ($n = 5$ repeats; 30 plants/repeat). Significant differences from REAT11 as determined by Student's *t*-test are shown (**$P < 0.01$). **d** SDS–PAGE (*left box*) and Western blot (*right box*) analyses. The protein Western blot was hybridized with the His antibody and detected with secondary antibody conjugated to horseradish peroxidase. Similar results were obtained in five of six experimental repetitions; the exception was provided in Fig. S3

free flavin content, respectively, owing to ectopic expression and silencing of the *TsRfBP* gene.

The TsRfBP protein localizes to chloroplasts and binds RIB

To gain information about the relationship between TsRfBP and changes of flavin content in the plant, subcellular localization of the protein and its activity to bind RIB were studied. According to a previous study (Hamajima and Ono 1995) and the online SignalP prediction (http://www.cbs.dtu.dk/services/signalp), TsRfBP possesses a signal peptide with the most likely cleavage site between C^{18} and K^{19} (C and K refer to cysteine and lysine; superscript numbers indicate the residue sites in the amino acid sequence). The online Predotar V1.03 program indicated TsRfBP localization to the endoplasmic reticulum, mitochondria, and the other cellular sites of the animal with 0.95, 0.06, and 0.104 possibilities (http://urgi.versailos.inta.tr/predoctar/prodoctar html). Quite surprisingly, the immune gold-silver probing assay conducted in this study detected TsRfBP in the chloroplast but not other cellular locations, such as the cell wall, plasma membrane, cytoplast, and mitochondria (Fig. 5a). Previously, the immune gold-silver probing assay was shown to be of much enhanced sensitivity (up to 200-fold) as compared with the conventional immunogold probing method (Holgate et al. 1983). To prevent the TsRfBP-gold-silver particles from crowding as found in our initial experiments, we used a low concentration TsRfBP antibody in combination with a low gold dose. The protocol offered a clear visualization of the immunogold-TsRfBP particles present

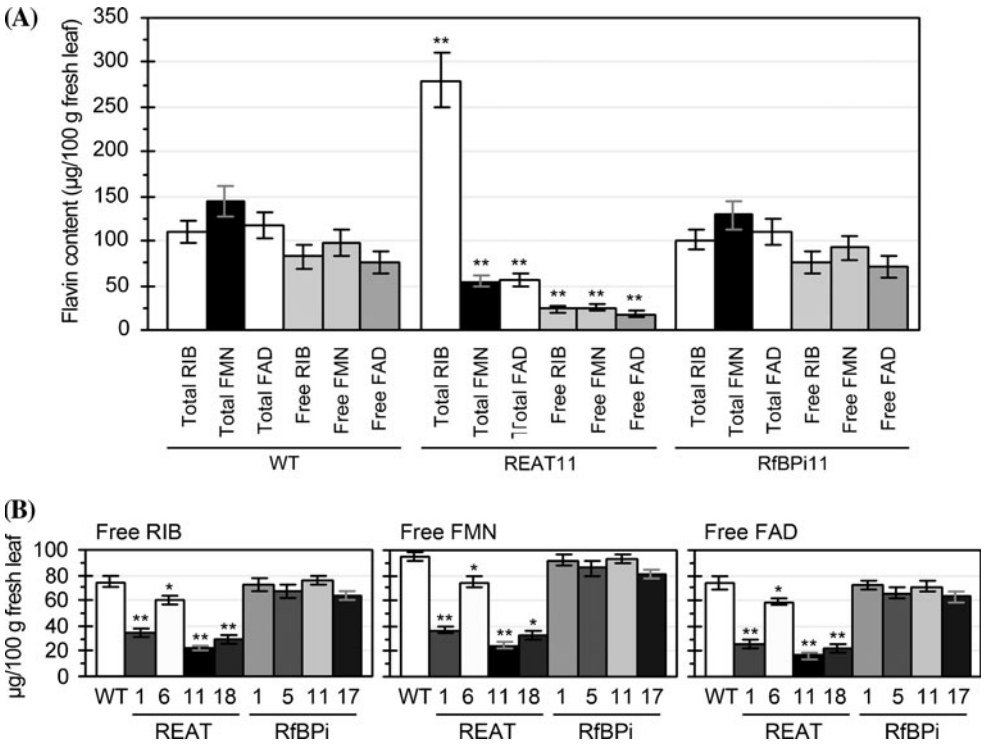

Fig. 4 Assays of flavins in plants. **a** Comparison of WT, REAT11, and RfBPi11 in leaf flavin content. **b** Comparison of WT, REAT lines, and RfBPi lines in levels of free flavins from leaves. In (**a**) and (**b**), data represent means ± SDs ($n = 3$ repeats, 30 plants/repeat), and significant differences from WT are indicated (*$P < 0.05$; **$P < 0.01$)

in chloroplasts of REAT11 and RfBPi11 rather than WT (Fig. 5a). The chloroplast localization of TsRfBP was confirmed by the conventional immunogold assay conducted with a higher concentration TsRfBP antibody in combination with a higher gold dosage. In this case, chloroplast stroma and thylakoid were well distinguished when majority of the immunogold-TsRfBP particles appeared in the lamina membrane (Fig. 5b). Both immunolocalization assays detected TsRfBP in REAT11 and RfBPi11 rather than WT (Fig. 5a, b). Consistently, the RIB-binding activity of TsRfBP evaluated versus plant weight was feeble when isolated from RfBPi11 but was much greater when isolated from REAT11 (Fig. 6; Fig. S4). The protein preparation from WT did not bind RIB, whereas, TsRfBP isolated from REAT11 was as active as the protein preparation from prokaryotic *TsRfBP* expression.

H_2O_2 is elevated owing to the ectopic *TsRfBP* expression

We studied the effect of the ectopic *TsRfBP* expression on ROS accumulation. The natural status of ROS was determined with water-treated plants. Levels of total ROS (Fig. 7a) and H_2O_2 (Fig. 7b), in particular, were elevated with H_2O_2 being 1.5 times more in REAT11 than in WT (Fig. 7b). As shown in Fig. 8a, increases of the H_2O_2 level were significant in the four REAT lines compared to WT (Student's *t*-test, $P < 0.01$). RfBPi differed from REAT11 in ROS accumulation. Observed levels of ROS (Fig. 7a) and H_2O_2 (Figs. 7b, 8a) were close in RfBPi and WT. In RfBPi11, amounts of ROS (Fig. 7a) and H_2O_2 (Fig. 7b) were smaller than in REAT11 but similar to those in WT (*ANOVA* test, $P < 0.01$). Therefore, the elevation of ROS was attributed to the ectopic *TsRfBP* expression.

To confirm the part of H_2O_2 in total ROS, plants were investigated following treatment with catalase, an H_2O_2 scavenger (Wang et al. 2009). The use of catalase markedly decreased accumulations of ROS (Fig. 7a) and H_2O_2 (Fig. 7b) in all plants but the changes varied with the plant genotype, especially for the content of H_2O_2. As shown in Fig. 7b, H_2O_2 declined greatly as the effect of catalase compared to water (Student's *t*-test, $P < 0.01$). The effect was greatest in REAT11 relative to WT and RfBPi11 based on statistical analyses applied to amounts of H_2O_2 decreased due to the use of catalase compared with water (*ANOVA* test, $P < 0.01$). Thus, H_2O_2 occupied a prominent proportion of ROS accumulated in the plant.

We next conducted histochemical assays by using fluorescent H_2O_2 probes AR and AUR to visualize H_2O_2 accumulation in the plant intracellular and extracellular spaces. In reaction with H_2O_2, AR and AUR are converted into resorufin and a resorufin analog, respectively, which emit strong crimson fluorescence (Ashtamker et al. 2007; Rhee et al. 2010). AR can penetrate the plasma membrane and thus probes H_2O_2 associated with the inner membrane and present in the intracellular space, whereas, AUR can not penetrate the plasma membrane and thus probes H_2O_2

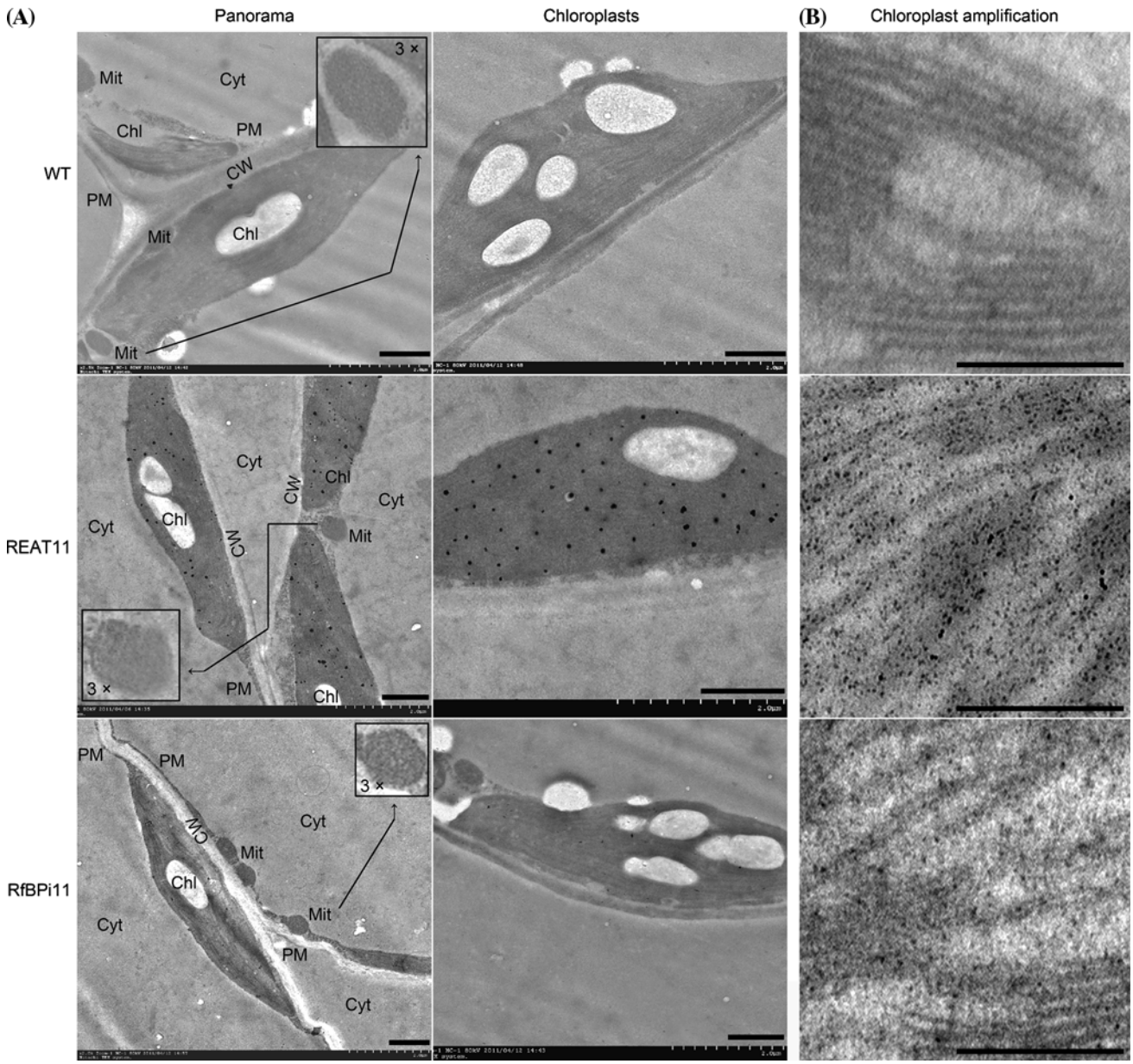

Fig. 5 Scanning electron microscopic images showing immunolocalization of TsRfBP in plant leaves. **a** Leaf ultrathin sections were probed with colloidal gold already tagged to the TsRfBP antiserum, and subsequently stained with a silver solution. *Chl* Chloroplast, *CW* Cell wall, *Cyt* Cytoplasm, *Mit* Mitochondria, *PM* Plasma membrane. *Scale bar*, 10 µm. **b** Leaf ultrathin sections were probed with colloidal gold tagged to the TsRfBP antiserum. *Scale bar*, 100 nm. The TsRfBP antiserum was used at a 1:50 titer in combination with a 5-nM gold colloid in (**a**) and a 1:20 titer in combination with a 10-nM gold colloid in (**b**). The titer determination was provided in Fig. 1c

present in the cell periphery, including the access to the outer membrane and the apoplastic space (Ashtamker et al. 2007; Šnyrychová et al. 2009; Rhee et al. 2010). When applied to *Arabidopsis* leaves, both AR and AUR were able to report H_2O_2 in contrast to the background of water-treated control (Fig. 7c). The H_2O_2 signal was stronger as reported by AR than by AUR, suggesting that H_2O_2 had a greater amount inside than outside the plant cell. Amounts of extracellular and intracellular H_2O_2 were close in RfBPi11 and WT but much greater in REAT11 (Fig. 7c).

REAT resistance to the bacterial pathogen is enhanced in a H_2O_2-dependent manner

To reveal if the ectopic *TsRfBP* expression induces pathogen defense in *Arabidopsis*, and to elucidate if H_2O_2 plays a role in the defense, plants were investigated following treatment with water or the H_2O_2 scavenger catalase and inoculation with DC3000. The bacterial population in plant tissues (Fig. 7d) was determined 3 d after inoculation. Two days later, the chlorosis and necrosis symptoms caused by the

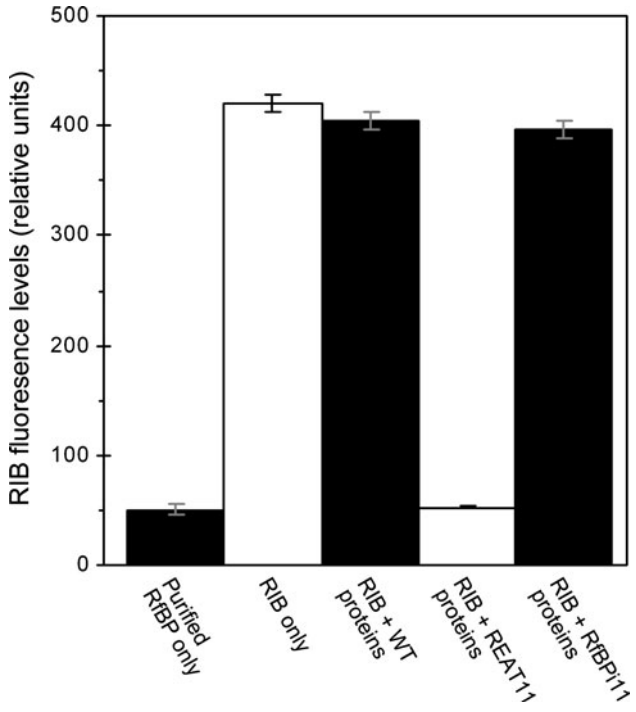

Fig. 6 Fluorescence quenching assay for RIB-binding activity of plant protein preparations. Each protein sample was incubated with an RIB solution and the mixture was observed by fluorescence microscopy. The RIB-binding activity was shown as decrease in fluorescence emitted from the protein-RIB complex compared to that eradiated by only RIB. The extent of RIB fluorescence was quantified with a spectrofluorometer. Data represent means ± SDs ($n = 3$ repeats; 30 plants/repeat). Colored images of RIB fluorescence were provided in Fig. S4

pathogen on leaves (Fig. 7e) were surveyed. Resistance was shown as decreased DC3000 population logarithm (Fig. 7d) and alleviated severities of the symptoms (Fig. 7e).

Based on the criteria, REAT11 was more resistant than WT to the pathogen, which had >1,500-fold greater population (Fig. 7d) and caused more severe symptoms (Fig. 7e) in WT than in REAT11, indicating resistance development in REAT11. Resistance was impaired in RfBPi11. RfBPi11 was similar to WT but both RfBPi11 and WT were inferior to REAT11 in resistance levels (Fig. 7d, e).

When catalase was applied to scavenge H_2O_2 (Fig. 7b), resistance levels in WT, REAT11, and RfBP11 were all decreased (Fig. 7d, e). The use of catalase significantly increased the *in planta* bacterial population (Fig. 7d) and aggravated severities of the symptoms (Fig. 7e). The effect of catalase to impair resistance was similar in WT and RfBPi11 but greater in REAT11 (Fig. 7d, e), suggesting the importance of H_2O_2 for resistance development in REAT11.

The level of H_2O_2 was further correlated with the level of resistance based on parallel tests of four REAT lines and four RfBPi lines in comparison with WT (Fig. 8). In these plants, variations of the spectrophotometric H_2O_2 content (Fig. 8a) were consistent with visible extents of AR-reported intracellular H_2O_2 signals (Fig. 8b, top photo panel). Greater or smaller amounts of H_2O_2 (Fig. 8a, b, top photo panel) were consistent with higher or lower extents by which DC3000 multiplication was repressed (Fig. 8b, histogram) in the REAT lines or the RfBPi lines compared with WT. Consistency was also found in H_2O_2 levels and the extents by which severities of the chlorosis and necrosis symptoms were alleviated (Fig. 8b, leaf photo panel). These comparisons confirmed that REAT11 was the strongest H_2O_2 producer and was the most resistant to the bacterial pathogen, suggesting that the pathogen defense in correlation with H_2O_2 production was a consistent character conferred by the ectopic *TsRfBP* expression.

H_2O_2 accumulation in REAT11 is independent of NADPH oxidase

To gain information on how RIB affects H_2O_2 and the pathogen defense, plants were investigated after treating with RIB, DPI (an NADPH oxidase inhibitor), a combination of both compounds, and water as a control. H_2O_2 accumulation (Fig. 9a) and DC3000 multiplication (Fig. 9b) were differently affected in WT, REAT11, and RfBPi11. Feeding WT and RfBPi11 with RIB caused an increase in the H_2O_2 level but a decrease in DC3000 multiplication. However, feeding with RIB did not have an evident effect on REAT11, suggesting that the extrinsic use of RIB did not compensate for the effect of down-regulated RIB. DPI diminishes H_2O_2 content by inhibiting NADPH oxidase activity (Riganti et al. 2004; Wang et al. 2009). Treatment with DPI resulted in decreases in H_2O_2 level and DC3000 population in WT and RfBPi11 but did not have an evident effect on REAT11. In REA11, neither H_2O_2 nor DC3000 was affected by the treatment with RIB, DPI or both. In WT and RfBPi11, however, DPI applied in combination with RIB impaired the effect of RIB. The externally applied RIB induced H_2O_2 in an NADPH oxidase-dependent manner, but the enzyme was not required for H_2O_2 accumulation in REAT11 (Fig. 9a). The pathogen defense, indicated by decreased DC3000 population (Dong et al. 1999), was constitutive in REAT11 but induced in WT and RfBPi11 (Fig. 9b).

Discussion

The developmental role of oviparous RfBPs in RIB binding and redistribution (Wasylewski 2000; Foraker et al. 2003; Latha et al. 2008) inspired the idea of manipulating plant RIB by using TsRfBP. Its activity in RIB binding (Fig. 1)

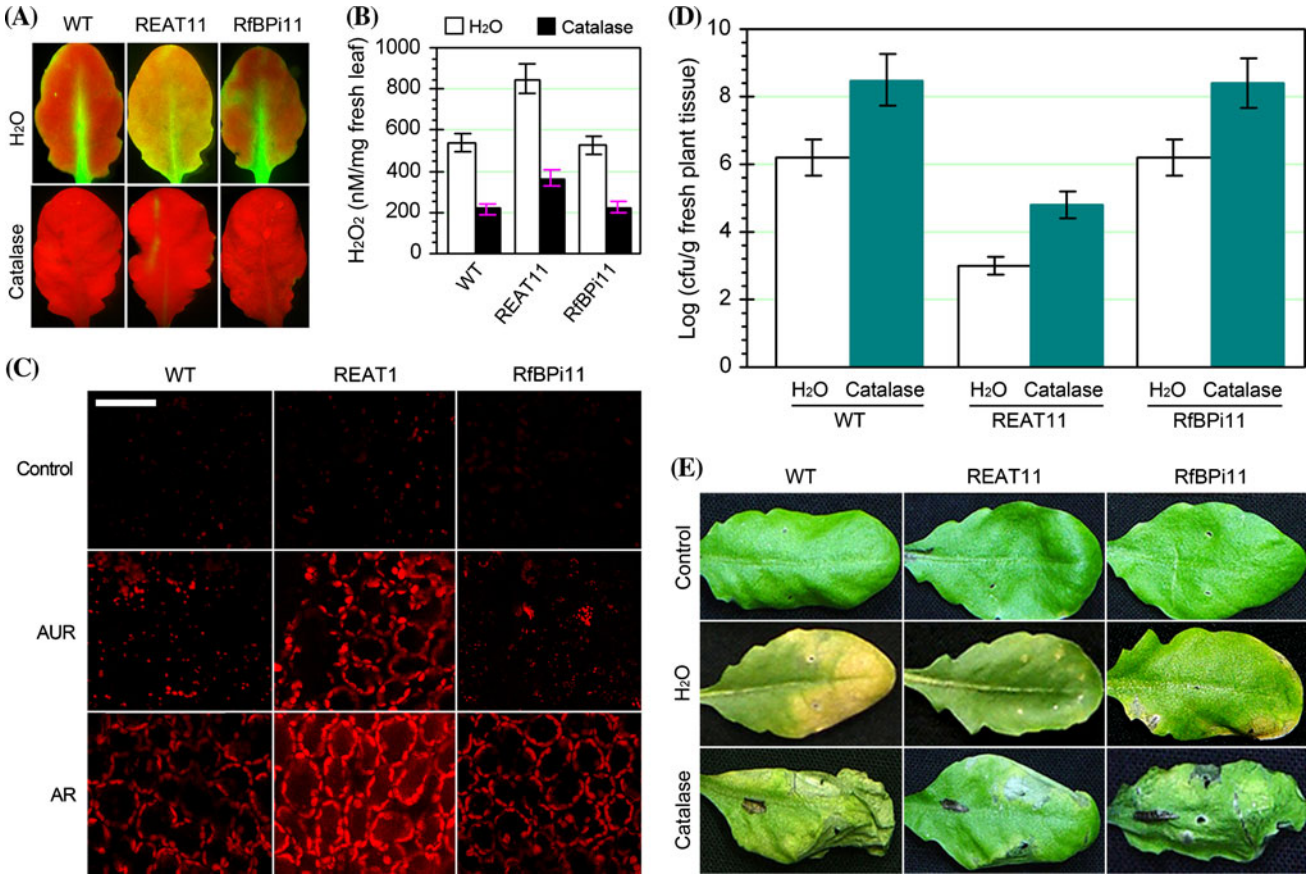

Fig. 7 Analyses of ROS and its effect on bacterial infection of the plant. **a** Visualization of ROS accumulated in leaves. Plants remained untreated or were treated by spraying with water or an aqueous solution of catalase. Twenty-four hours later, ROS in leaves was visualized as green fluorescence by staining with 2, 7-dichlorofluorescein diacetate. **b** Spectrophotometric H_2O_2 content in leaves 24 h after treatment from (**a**). **c** Visualization H_2O_2 in leaf epidermal cells. Plant leaves remained untreated (control) and treated with the H_2O_2 probe AR or AUR were observed with a laser scanning confocal microscope. AR and AUR reported H_2O_2 as crimson fluorescence under black background. *Scale bar*, 50 μm. **d** and **e** Evaluation of the plant response to the bacterial pathogen *P. syringae* pv. *tomato* DC3000 (DC3000). Plants remained untreated or were treated with water and catalase, respectively, and inoculated 5 days later. **d** DC3000 population recovered from plants 3 days after inoculation and scored as logarithmic (Log) value of colony formation unit (cfu). **e** Leaves photographed 5 days after inoculation. In (**b**) and (**d**), data represent means ± SDs ($n = 3$ repeats; 30 plants/repeat)

provides a basis for the *TsRfBP* gene to function in transgenic plants. We have introduced *TsRfBP* into *Arabidopsis*, generated several REAT lines including REAT11 (Fig. 2), and created RfBPi plants by a *TsRfBP*-silencing protocol applied to REAT11 (Fig. 3). Consistent with previous evidence that the use of distant genes is an effective way to enrich plant genetic diversity and defensive arsenal (Stuiver and Custers 2001), the ectopic expression of *TsRfBP* alters the pathogen defense in relation to the changes of intrinsic flavin levels. Leaf content of free flavins is down-regulated in REAT, whereas, RfBPi plants regain the WT character in the flavin content (Fig. 4). These results suggest that the manipulation of RIB by ectopic *TsRfBP* expression is capable of modulating the intrinsic flavin content.

Our experimental evidence that TsRfBP localizes to the chloroplast (Fig. 5) poses a difficulty to understanding how the animal protein behaves in transgenic plants. The result is inconsistent with the predicted priority of TsRfBP localization to endoplasmic reticulum over several other locations in the animal cell. It is intuitional to think that the protein may have an unknown signal peptide or use an unknown signal from plants. Alternatively, the cellular sites of RIB biosynthesis could dictate TsRfBP localization. In plants, RIB is speculated to be synthesized mainly in the plastid, a precursor of the chloroplast and other organelles, and complies with the developmental requirement for translocation to cytoplast and different organelles (Sandoval and Roje 2005; Giancaspero et al. 2009). It is possible that RIB binding or the binding-directed movement of TsRfBP serves as a force that impels the protein to anchor on the chloroplast. This localization permits the possibility for TsRfBP binding of RIB in the correct location predicted for the biosynthesis of RIB and reactions

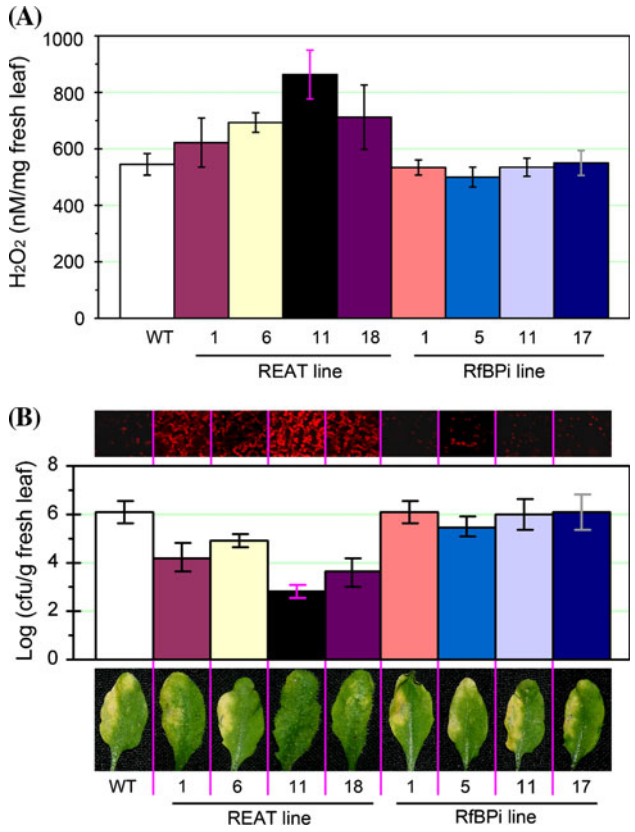

Fig. 8 Comparisons of WT and different lines of REAT and RfBPi in terms of H_2O_2 accumulation and in response to DC3000 inoculation. **a** Spectrophotometric H_2O_2 content in plant leaves. **b** AR-reported H_2O_2 in leaves (*top photo panel*), the *in planta* DC3000 population recovered from leaves 3 days after inoculation (*histogram panel*), and leaves photographed 5 days after inoculation (*bottom photo panel*). Histograms in (**a**) and (**b**) represent means ± SDs ($n = 5$ repeats; 30 plants/repeat)

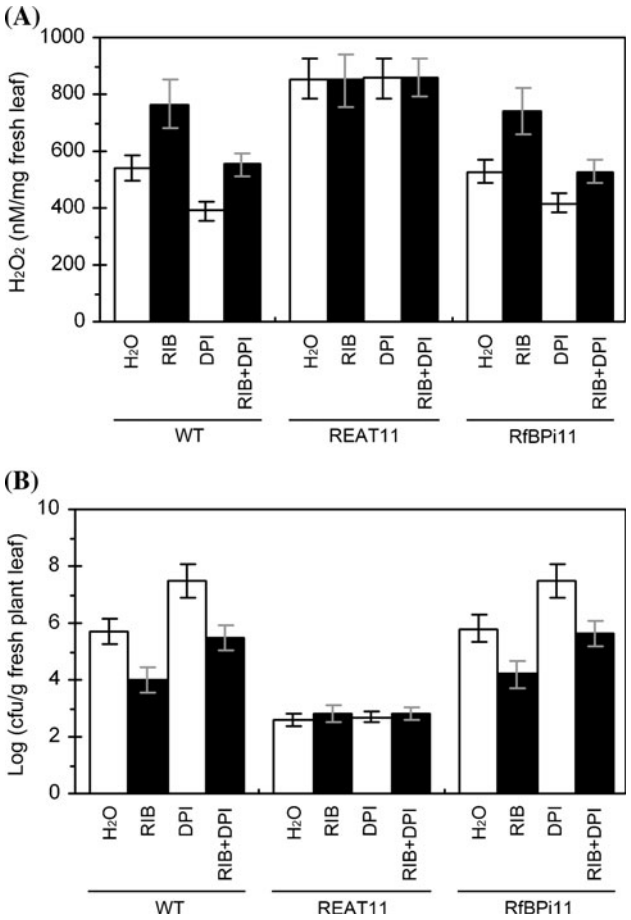

Fig. 9 Different effects of the external application of RIB and diphenyleneiodonium (DPI) on H_2O_2 accumulation and DC3000 multiplication in WT, REAT11, and RfBPi11. **a** Plants were treated with water in control and the indicated compounds, respectively. Two days later, concentrations of H_2O_2 were determined by spectrophotometric analysis. **b** Plants from (**a**) were inoculated with a DC3000 suspension 5 days after treatment. Three days later, the bacterial population was determined. In (**a**) and (**b**), data represent means ± SDs ($n = 3$ experimental repeats; 30 plants/repeat)

of flavin form conversions (Herz et al. 2000; Sandoval and Roje 2005). This possibility was found in prominent RIB-binding activity of the TsRfBP protein isolated from REAT11 (Fig. 6), consistent with the sharp increase in bound RIB in the plant (Fig. 4). The coincident decreases in levels of free flavins conform to dynamics of flavin form conversions. RIB and FMN conversion is reversible (Sandoval and Roje 2005), while FMN to FAD conversion is irreversible (Hersh and Walsh 1980). Accumulation of a particular flavin is concentration dependent, so a smaller amount of free RIB or FMN results in a smaller amount of FMN or FAD (Weimar and Neims 1975). Thus, down-regulation of free RIB is a cause of coordinate decreases of free FMN and FAD content in the plant.

The decrease in free flavin content has significant impacts on the production of ROS and defense response in the plant (Figs. 7, 8, and 9). The elevation of H_2O_2 and total ROS levels (Fig. 7) concomitant with decreases in free flavins (Fig. 4) is accordant with biochemical functions of flavins, especially FMN and FAD, in regulation of cellular redox (Jordan et al. 1999). Our evidence supports that H_2O_2 elevated due to the ectopic *TsRfBP* expression plays a role in plant resistance to the bacterial pathogen. According to previous studies, H_2O_2 is either dispensable or indispensable for plant defenses under different circumstances (Wang et al. 2009). In this study, the importance of H_2O_2 for defense response has been found in the function of catalase to coincidently scavenge H_2O_2 and inhibit plant resistance (Fig. 7). Behaviors of the different REAT lines and RfBPi lines suggest that the H_2O_2-resistance concomitancy is a consistent character conferred by the ectopic *TsRfBP* expression (Fig. 8). Like REAT, the *Arabidopsis* mutant *cos1* is arrested in RIB biosynthesis, and has lower RIB content and higher level of resistance to pathogens (Xiao et al. 2004). Therefore, modulation of the

intrinsic RIB content plays a role in pathogen defense of plants.

As reported by AR and AUR, the much recently developed H_2O_2 probes that have been used only in a few cases of the plant study, H_2O_2 is distributed at least partially inside the plant cell (Figs. 7 and 8). AR is a commercial name of 10-acetyl-3, 7-dihydroxyphenoxazine, a colorless, non-fluorescent derivative of dihydro-resorufin (7-hydroxy-3H-phenoxazin-3-one), which produces the highly fluorescent resorufin in a peroxidase-catalytic reaction with H_2O_2 (Ashtamker et al. 2007; Rhee et al. 2010). AUR is an improved version of AR with enhanced sensitivity and better stability. In a peroxidase-catalytic reaction with H_2O_2, AUR is converted into a resorufin analog that is also highly fluorescent (Ashtamker et al. 2007; Šnyrychová et al. 2009). Excitation and emission maxima of resorufin do not overlap with the spectral features of chlorophylls (Ashtamker et al. 2007; Šnyrychová et al. 2009; Rhee et al. 2010), allowing for specific detection of H_2O_2 in plant leaves (Šnyrychová et al. 2009). Like the spectrophotometric H_2O_2, H_2O_2 reported by AR or AUR is also in consistence with plant resistance (Figs. 7 and 8) although at present we do not have evidence to show the intracellular or extracellular proportion. This requires studies by using more specific techniques, such as spectrofluorometry (Ashtamker et al. 2007; Šnyrychová et al. 2009), or more accurately, monitoring of the apoplastic-cytoplasmic translocation of H_2O_2 subsequent to generation from the extracellular and intracellular sources (Torres 2010). The supposed H_2O_2 translocation may not depend on free diffusion, but instead, it may comply with certain modes of the selectivity (Ludewig and Dynowski 2009; Hachez and Chaumont 2010). Importantly, the aquaporin channel essential for water uptake (Cramer et al. 2009; Gomes et al. 2009; Knipfer et al. 2011) is implicated in the cellular translocation of other small compounds (Ali et al. 2009; Verbruggen et al. 2009) including H_2O_2 (Ludewig and Dynowski 2009; Hooijmaijers et al. 2011) in plants. It is likely that the involvement of aquaporin in pathogen defenses (Shirasu et al. 1999; Marulanda et al. 2010) and drought tolerance (Almeida-Rodriguez et al. 2010; Kline et al. 2010) of plants may be attributable to apoplastic-cytoplasmic transduction of defense signals. This hypothesis is related to the trafficking of H_2O_2 and other types of ROS from different pools in plants (Torres 2010).

ROS generated by different mechanisms, such as activities of NADPH oxidases (Torres 2010) and electron leakage from the mitochondrial electron transport chain (Noctor et al. 2007), contributes similarly to the phenotype of pathogen defense (Torres 2010). This notion is also supported by our result (Fig. 9). The extrinsic application of RIB to WT and RfBPi11 induces H_2O_2 in an NADPH oxidase-dependent manner. Inversely, the enzyme is not likely to take a part in H_2O_2 accumulation due to down-regulation of the intrinsic flavins. It is interesting to study in the future whether the mitochondrial electron transport chain is a source of ROS generation in REAT plants. In the mitochondrial electron transport chain, electron leakage results from blocks in electron channeling via complex I through complex III while complex I and complex III use FMN and FAD, respectively, as redox centers (Lenaz et al. 2006). Changes in the intrinsic flavin content may have pivotal effects on electron leakage, H_2O_2 generation, and pathogen defenses. This hypothesis remains to be tested.

Overall, our results suggest that down-regulation of free flavins is responsible for the elevation of H_2O_2 and the development of plant resistance to the bacterial pathogen. However, defense response is not the only plant trait acquired due to the ectopic *TsRfBP* expression. We have unexpectedly observed different phenotypic variations in REAT from WT. For example, REAT lines with enhanced resistance to *P. syringae* all flower earlier than WT, and all RfBPi lines with retrieved WT resistance character also regain the character of flowering as regular as in WT. When growing in short day, RIRA11 has 6 less rosette leaves at the first flowering day and flowers 22 days earlier than WT or RfBPi11. The remarkable difference is beyond our initial purpose to study the effect of modulating flavins, RIB in particular, on plant resistance to pathogens (Dong and Beer 2000; Zhang et al. 2009; Deng et al. 2010). Thus, we have taken a long period study, since the generation of REAT plants in 2002, seeking experimental evidence that can elucidate a molecular basis of the early flowering character. Of especial significance, REAT11 has enhanced expression of the floral identity genes *FD* and *AP1*, integrators of the several floral pathways (Abe et al. 2005), in consistence with H_2O_2 generation via electron leakage from the mitochondrial electron transport chain. These observations at least suggest that the ectopic production of the TsRfBP protein might have other unforeseen effects beyond binding RIB. The linkages between the floral transition pathways (Corbesier and Coupland 2006), H_2O_2, and the ectopic *TsRfBP* expression will be the subject of future studies.

Acknowledgments We appreciate technical assistance provided by Dr. Shuping Qu, a former postdoctoral fellow, and former graduate students Dr. Ganyu Gu, Miss Yuxing Liu, Miss Ying Wang, and Miss Zhenzhu Xiahou, who were studying during 2001–2006 in the laboratory. We thank Miss Junzi Dong (Department of Biomedical Engineering, Washington University in St. Louis) for reading of the manuscript. This study was supported by grants from China National Novel Transgenic Organisms Breeding Projects (2009ZX08002-004B and 2008ZX08002-001) and the Priority Academic Program Development of Jiangsu Higher Education Institutions.

References

Abe M, Kobayashi Y, Yamamoto S, Daimon Y, Yamaguchi A, Ikeda Y, Ichinoki H, Notaguchi M, Goto K, Araki T (2005) FD, a bZIP protein mediating signals from the floral pathway integrator FT at the shoot apex. Science 309:1052–1056

Adiga PR, Visweswariah SS, Karande AA, Velu NK (1988) Biochemical and immunological aspects of riboflavin carrier protein. J Biosci 13:87–104

Ali W, Isayenkov SV, Zhao FJ, Maathuis FJ (2009) Arsenite transport in plants. Cell Mol Life Sci 66:2329–2339

Allan AC, Fluhr R (1997) Two distinct sources of elicited reactive oxygen species in tobacco epidermal cells. Plant Cell 9:1559–1572

Almeida-Rodriguez AM, Cooke JE, Yeh F, Zwiazek JJ (2010) Functional characterization of drought-responsive aquaporins in *Populus balsamifera* and *Populus simonii* × *balsamifera* clones with different drought resistance strategies. Physiol Plant 140: 321–333

Asai S, Mase K, Yoshioka H (2010) A key enzyme for flavin synthesis is required for nitric oxide and reactive oxygen species production in disease resistance. Plant J 62:911–924

Ashtamker C, Kiss V, Sagi M, Davydov O, Fluhr R (2007) Diverse subcellular locations of crytogein-induced reactive oxygen species production in tobacco bright yellow-2 cells. Plant Physiol 143:1817–1826

Bacher A, Eberhardt S, Eisenreich W, Fischer M, Herz S, Illarionov B, Kis K, Richter G (2001) Biosynthesis of riboflavin. Vitam Horm 61:1–49

Bartosík M, Ostatná V, Palecek E (2009) Electrochemistry of riboflavin-binding protein and its interaction with riboflavin. Bioelectrochemistry 76:70–75

Bedhomme M, Hoffmann M, McCarthy EA, Gambonnet B, Moran RG, Rébeillé F, Ravanel S (2005) Folate metabolism in plants: an *Arabidopsis* homolog of the mammalian mitochondrial folate transporter mediates folate import into chloroplasts. J Biol Chem 280:34823–34831

Binet MN, Humbert C, Lecourieux D, Vantard M, Pugin A (2001) Disruption of microtubular cytoskeleton induced by cryptogein, an elicitor of hypersensitive response in tobacco cells. Plant Physiol 125:564–572

Blankenhorn G (1978) Riboflavin binding in egg-white flavoprotein: the role of tryptophan and tyrosine. Eur J Biochem 82:155–160

Chen Z, Silva H, Klessig D (1993) Involvement of reactive oxygen species in the induction of systemic acquired resistance by salicylic acid in plants. Science 242:883–886

Chen L, Qian J, Qu S, Long J, Yin Q, Zhang C, Wu X, Sun F, Wu T, Hayes M, Beer SV, Dong H (2008) Identification of specific fragments of $HpaG_{Xooc}$, a harpin from *Xanthomonas oryzae* pv. *oryzicola*, that induce disease resistance and enhance growth in plants. Phytopathology 98:781–791

Corbesier L, Coupland G (2006) The quest for florigen: a review of recent progress. J Exp Bot 57:3395–3403

Cramer MD, Hawkins HJ, Verboom GA (2009) The importance of nutritional regulation of plant water flux. Oecologia 161:15–24

Dawson KR, Unklesbay NF, Hedrick HB (1988) HPLC determination of riboflavin, niacin, and thiamin in beef, pork, and lamb after alternate heat-processing methods. J Agric Food Chem 36: 1176–1179

de Souza AC, Kodach L, Gadelha FR, Bos CL, Cavagis AD, Aoyama H, Peppelenbosch MP, Ferreira CV (2006) A promising action of riboflavin as a mediator of leukaemia cell death. Apoptosis 11:1761–1771

Deng S, Yu M, Wang Y, Jia Q, Lin L, Dong H (2010) The antagonistic effect of hydroxyl radical on the development of a hypersensitive response in tobacco. FEBS J 277:5097–5111

Dong H, Beer SV (2000) Riboflavin induces disease resistance in plants by activating a novel signal transduction pathway. Phytopathology 90:801–811

Dong H, Delaney TP, Bauer DW, Beer SV (1999) Harpin induces disease resistance in *Arabidopsis* through the systemic acquired resistance pathway mediated by salicylic acid and the *NIM1* gene. Plant J 20:207–215

Dong H, Yu H, Bao Z, Guo X, Peng J, Yao Z, Chen G, Qu S, Dong H (2005) The *ABI2*-dependent abscisic acid signalling controls HrpN-induced drought tolerance in *Arabidopsis*. Planta 221: 313–327

Fernandez AP, Strand A (2008) Retrograde signaling and plant stress: plastid signals initiate cellular stress responses. Curr Opin Plant Biol 11:509–513

Foraker AB, Khantwal CM, Swaan PW (2003) Current perspectives on the cellular uptake and trafficking of riboflavin. Adv Drug Deliv Rev 55:1467–1483

Frens G (1973) Controlled nucleation for the regulation of the particle size in monodisperse gold solution. Nat Physic Sci 241:20–22

Gajewska E, Sklodowska M (2007) Effect of nickel on ROS content and antioxidative enzyme activities in wheat leaves. Biometals 20:27–36

Gastaldi G, Laforenza U, Casirola D, Ferrari G, Tosco M, Rindi G (1999) Energy depletion differently affects membrane transport and intracellular metabolism of riboflavin taken up by isolated rat enterocytes. J Nutr 129:406–409

Giancaspero TA, Locato V, de Pinto MC, De Gara L, Barile M (2009) The occurrence of riboflavin kinase and FAD synthetase ensures FAD synthesis in tobacco mitochondria and maintenance of cellular redox status. FEBS J 276:219–231

Gomes D, Agasse A, Thiébaud P, Delrot S, Gerós H, Chaumont F (2009) Aquaporins are multifunctional water and solute transporters highly divergent in living organisms. Biochim Biophys Acta 1788:1213–1228

Guevara I, Zak Z (1993) Fluorescence quenching in riboflavin-binding protein and its complex with riboflavin. J Protein Chem 12:179–185

Hachez C, Chaumont F (2010) Aquaporins: a family of highly regulated multifunctional channels. Adv Exp Med Biol 679:1–17

Hamajima S, Ono S (1995) Sequence of a cDNA encoding turtle riboflavin-binding protein: a comparison with avian riboflavin-binding protein. Gene 164:279–282

Hersh LB, Walsh C (1980) Preparation, characterization, and coenzymic properties of 5-Carba-5-deaza and 1-Carba-1-deaza analogs of riboflavin, FMN and FAD. In: McCormick DB, Wright LD (eds) Vitamins and coenzymes. Academic Press, New York, pp 277–287

Herz S, Eberhardt S, Bacher A (2000) Biosynthesis of riboflavin in plants. The ribA gene of Arabidopsis thaliana specifies a bifunctional GTP cyclohydrolase II/3, 4-dihydroxy-2-butanone 4-phosphate synthase. Phytochemistry 53:723–731

Hodges GM, Smolira MA, Livingston DC (1984) Scanning electron microscope immuno-cytochemistry in practice. In: Polak J, Varndell I (eds) Immunolabelling for electron microscopy. Elsevier, Amsterdam, pp 189–233

Holgate CS, Jackson P, Cowen PN, Bird CC (1983) Immunogold-silver staining: new method of immunostaining with enhanced sensitivity. J Histochem Cytochem 31:938–944

Hooijmaijers C, Rhee JY, Kwak KJ, Chung GC, Horie T, Katsuhara M, Kang H (2011) Hydrogen peroxide permeability of plasma membrane aquaporins of *Arabidopsis thaliana*. J Plant Res 69:3723−3726

Huang SN, Swaan PW (2000) Involvement of a receptor-mediated component in cellular translocation of riboflavin. J Pharmacol Exp Ther 294:117–125

Jiang M, Zhang J (2001) Effect of abscisic acid on active oxygen species, antioxidative defense system and oxidative damage in leaves of maize seedlings. Plant Cell Physiol 42:1265–1273

Jordan DB, Bacot KO, Carlson TJ, Kessel M, Viitanen PV (1999) Plant riboflavin biosynthesis. Cloning, chloroplast localization, expression, purification, and partial characterization of spinach lumazine synthase. J Biol Chem 274:22114–22121

Kline KG, Barrett-Wilt GA, Sussman MR (2010) *In planta* changes in protein phosphorylation induced by the plant hormone abscisic acid. Proc Natl Acad Sci USA 107:15986–15991

Knipfer T, Besse M, Verdeil JL, Fricke W (2011) Aquaporin-facilitated water uptake in barley (*Hordeum vulgare* L.) roots. J Exp Bot. doi: 10.1093/jxb/err075

Kozik A (1982) Disulfide bonds in egg-white riboflavin-binding protein: chemical reduction studies. Eur J Biochem 121:395–400

Latha M, Bangaru Y, Karande AA (2008) Biochemical characterization of recombinant chicken riboflavin carrier protein. Mol Cell Biochem 308:1–7

Lenaz G, Fato R, Genova ML, Bergamini C, Bianchi C, Biondi A (2006) Mitochondrial complex I: structural and functional aspects. Biochim Biophys Acta 1757:1406–1420

Levine A, Tenhaken R, Dixon R, Lamb C (1994) H_2O_2 from the oxidative burst orchestrates the plant hypersensitive disease resistance response. Cell 79:583–593

Liu F, Liu H, Jia Q, Wu X, Guo X, Zhang S, Song F, Dong H (2006) The internal glycine-rich motif and cysteine suppress several effects of $HpaG_{Xooc}$ in plants. Phytopathology 96:1052–1059

Liu R, Lü B, Wang X, Zhang C, Zhang S, Qian J, Chen L, Shi H, Dong H (2010) Thirty-seven transcription factor genes differentially respond to a harpin protein and affect resistance to the green peach aphid in Arabidopsis. J Biosci 35:435−450

Livak KJ, Schmittgen TD (2001) Analysis of relative gene expression data using real-time quantitative PCR and the $2^{-\Delta\Delta C}_{T}$. Method. Methods 25:402–408

Lorenz A, Kaldenhoff R, Hertel R (2003) A major integral protein of the plant plasma membrane binds flavin. Protoplasma 221:19–30

Ludewig U, Dynowski M (2009) Plant aquaporin selectivity: where transport assays, computer simulations and physiology meet. Cell Mol Life Sci 66:3161–3175

Maehashi K, Matano M, Uchino M, Yamamoto Y, Takano K, Watanabe T (2009) The primary structure of a noval riboflavin-binding protein of emu (*Dromaius novaehollandiae*). Comp Biochem Physiol (Part B) 153:95–100

Marulanda A, Azcón R, Chaumont F, Ruiz-Lozano JM, Aroca R (2010) Regulation of plasma membrane aquaporins by inoculation with a Bacillus megaterium strain in maize (*Zea mays* L.) plants under unstressed and salt-stressed conditions. Planta 232:533–543

Monaco HL (1997) Crystal structure of chicken riboflavin-binding protein. EMBO J 16:1475–1483

Mori T, Sakurai E (1996) Riboflavin affects anthocyanin synthesis in nitrogen culture using strawberry suspended cells. J Food Sci 61:698–702

Natraj U, George S, Kadam PA (1988) Isolation and partial characterization of human riboflavin carrier protein and the estimation of this protein during human pregnancy. J Reprod Immunol 13:1–16

Noctor G, De Paepe R, Foyer CH (2007) Mitochondrial redox biology and homeostasis in plants. Trends Plant Sci 12:125–134

Orrenius S, Gogvadze V, Zhivotovsky B (2007) Mitochondrial oxidative stress: implications for cell death. Annu Rev Pharmacol Tox 47:143–183

Paranagama MP, Sakamoto K, Amino H, Awano M, Miyoshi H, Kita K (2010) Contribution of the FAD and quinone binding sites to the production of reactive oxygen species from *Ascaris suum* mitochondrial complex II. Mitochondrion 10:158–165

Peng J, Dong H, Dong H, Delaney TP, Bonasera BM, Beer SV (2003) Harpin-elicited hypersensitive cell death and pathogen resistance requires the *NDR1* and *EDS1* genes. Physiol Mol Plant Pathol 62:317–326

Peng J, Bao Z, Ren H, Wang J, Dong H (2004) Expression of $harpin_{Xoo}$ in transgenic tobacco induces pathogen defense in the absence of hypersensitive cell death. Phytopathology 94: 1048–1055

Piacenza L, Irigoín F, Alvarez MN, Peluffo G, Taylor MC, Kelly JM, Wilkinson SR, Radi R (2007) Mitochondrial superoxide radicals mediate programmed cell death in *Trypanosoma cruzi*: cytoprotective action of mitochondrial iron superoxide dismutase overexpression. Biochem J 403:323–334

Powers HJ (2003) Riboflavin (vitamin B-2) and health. Am J Clin Nutr 77:1352–1360

Rancy PC, Thorpe C (2008) Oxidative protein folding in vitro: a study of the cooperation between quiescin-sulfhydryl oxidase and protein disulfide isomerase. Biochemistry 47:12047–12056

Rhee SG, Chang T-S, Jeong W, Kang D (2010) Methods for detection and measurement of hydrogen peroxide inside and outside of cells. Mol Cells 29:539–549

Rhodes MB, Bennett N, Feeney RE (1959) The flavoprotein-apoprotein system of egg white. J Biol Chem 234:2054–2060

Riganti C, Gazzano E, Polimeni M, Costamagna C, Bosia A, Ghigo D (2004) Diphenyleneiodonium inhibits the cell redox metabolism and induces oxidative stress. J Biol Biochem 279:47726–47731

Roje S (2007) Vitamin B biosynthesis in plants. Phytochemistry 68:1904–1921

Sabharanjak S, Mayor S (2004) Folate receptor endocytosis and trafficking. Adv Drug Deliv Rev 56:1099–1109

Said HM, Mohammed ZM (2006) Intestinal absorption of water-soluble vitamins: an update. Curr Opin Gastroen 22:140–146

Sandoval FJ, Roje S (2005) An FMN hydrolase is fused to a riboflavin kinase homolog in plants. J Biol Chem 280:38337–38345

Sasabe M, Takeuchi K, Kamoun S, Ichinose Y, Govers F, Toyoda K, Shiraishi T, Yamada T (2000) Independent pathways leading to apoptotic cell death, oxidative burst and defense gene expression in response to elicitin in tobacco cell suspension culture. Eur J Biochem 267:5005–5013

Shirasu K, Lahaye T, Tan M-W, Zhou F, Azevedo C, Schulze-Lefert P (1999) A novel class of eukaryotic zinc-binding proteins is required for disease resistance signaling in barley and development in *C. elegans*. Cell 99:355–366

Sierra I, Vidal-Valverde C (1999) Kinetics of free and glycosylated B6 vitamers, thiamin and riboflavin during germination of pea seeds. J Sci Food Agr 79:307–310

Šnyrychová I, Ayaydin F, Hideg É (2009) Detecting hydrogen peroxide in leaves in vivo—a comparison of methods. Physiol Plant 135:1–18

Sooryanarayana K, Sarkar S, Adiga PR, Visweswariah SS (1998) Identification and characterization of receptors for riboflavin carrier protein in the chicken oocyte. Role of the phosphopeptide in mediating receptor interaction. Biochim Biophys Acta 1382: 230–242

Storey KB, Dent ME, Storey JM (1999) Gene expression during estivation in spadefoot toads, *Scaphiopus couchii*: upregulation of riboflavin binding protein in liver. J Exp Zool 284:325–333

Stuiver MH, Custers J (2001) Engineering disease resistance in plants. Nature 411:865–868

Sun L, Ren H, Liu R, Li B, Wu T, Sun F, Liu H, Wang X, Dong H (2010) An h-type thioredoxin functions in tobacco defense responses to two species of viruses and an abiotic oxidative stress. Mol Plant-Microbe Interact 23:1470–1485

Taheri P, Höfte M (2006) Riboflavin induces resistance in rice against *Rhizoctonia* sheath diseases by activating signal transduction pathways leading to upregulation of rice cationic peroxidase and

formation of lignin as a structural barrier. Commun Agr Appl Biol Sci 71:255–258

Taheri P, Tarighi S (2010) Riboflavin induces resistance in rice against *Rhizoctonia solani* via jasmonate-mediated priming of phenylpropanoid pathway. J Plant Physiol 167:201–208

Torres MA (2010) ROS in biotic interactions. Physiol Plant 138:414–429

Torres MA, Jones JD, Dangl JL (2006) Reactive oxygen species signaling in response to pathogens. Plant Physiol 141:373–378

Trouvelot S, Varnier AL, Allegre M, Mercier L, Baillieul F, Arnould C, Gianinazzi-Pearson V, Klarzynski O, Joubert JM, Pugin A, Daire X (2008) A β-1, 3 glucan sulphate induces resistance in grapevine against Plasmopara viticola through priming of defense responses, including HR like cell death. Mol Plant-Microbe Interact 21:232–243

Verbruggen N, Hermans C, Schat H (2009) Mechanisms to cope with arsenic or cadmium excess in plants. Curr Opin Plant Biol 12:364–372

Vorwieger A, Gryczka C, Czihal A, Douchkov D, Tiedemann J, Mock HP, Jakoby M, Weisshaar B, Saalbach I, Bäumlein H (2007) Iron assimilation and transcription factor controlled synthesis of riboflavin in plants. Planta 226:147–158

Wang DS, Senthilkumaran B, Kobayashi T, Kajiura-Kobayashi H, Matsuda M, Yoshikuni M, Nagahama Y (2003) Molecular cloning and gene expression of the riboflavin-binding protein in the Nile tilapia, *Oreochromis niloticus*. Fish Physiol Biochem 28:225–226

Wang Y, Liu R, Chen L, Wang Y, Liang Y, Wu X, Li B, Wu J, Wang X, Zhang C, Wang Q, Hong X, Dong H (2009) *Nicotiana tabacum* TTG1 contributes to ParA1-induced signalling and cell death in leaf trichomes. J Cell Sci 122:2673–2685

Wasylewski M (2000) Binding study of riboflavin-binding protein with riboflavin and its analogues by differential scanning calorimetry. J Protein Chem 19:523–528

Weimar WR, Neims AH (1975) Physical and Chemical Properties of flavin. In: Rivlin RS (ed) Riboflavin. Plenum Press, New York, pp 2–36

Wu T, Guo A, Zhao Y, Wang M, Wang Y, Zhao D, Li X, Ren H, Dong H (2010) Ectopic expression of the rice lumazine synthase gene contributes to defense responses in transgenic tobacco. Phytopathology 100:573–581

Xiao S, Dai L, Liu F, Wang Z, Peng W, Xie D (2004) COS1: an *Arabidopsis coronatine insensitive1* suppressor essential for regulation of jasmonate-mediated plant defense and senescence. Plant Cell 16:1132–1142

Zhang SJ, Yang X, Sun MW, Sun F, Deng S, Dong H (2009) Riboflavin-induced priming for pathogen defense in *Arabidopsis thaliana*. J Integr Plant Biol 51:167–174

Zheng DB, Lim HM, Pene JJ, White HB (1988) Chicken riboflavin-binding protein cDNA sequence and homology with milk folate-binding protein. J Biol Chem 263:11126–11129